Charge Transport in Solid and Liquid Ar, Kr, and Xe

L. S. MILLER, S. HOWE, AND W. E. SPEAR
Physics Department, University of Leicester, Leicester, England
(Received 25 September 1967)

This paper reports an investigation of the drift velocity of excess electrons in solid and liquid Ar, Kr, and Xe. After purification of the commercially available gas, thin crystal specimens (100–600 μm) were grown from the liquid between parallel electrodes in a chamber attached to a miniature cryostat. Pulses of 40-keV electrons were used to generate the charge carriers in both liquids and solids. This technique overcomes the limitations inherent in previously applied methods and has made it possible to investigate the drift velocity over a range of applied fields from 10 V cm^{-1} to 100 kV cm^{-1}. Near the triple point, the low-field mobility μ_0 in solid Ar, Kr, and Xe was found to be 1000, 3700, and about 4500 cm^{2}sec^{-1}V^{-1}, respectively. In the liquids the corresponding mobilities were 475, 1800, and 2200 cm^{2}sec^{-1}V^{-1}. The temperature dependence of μ_0 has been measured on Ar crystals, and the results indicate that μ_0 is determined by acoustic scattering. The electron lifetime appears to be controlled predominantly by oxygen impurities. Pronounced hot-electron effects are observed in drift-velocity–versus–field curves for both liquids and solids, and their fit to the Shockley hot-electron theory has been investigated. In the high-field region all the curves show an almost complete saturation with field. The theory of Cohen and Lekner applied to liquid Ar fits the results over most of the field range, suggesting that the deviations from the Shockley theory at higher electron temperatures are associated with an increase in the value of the structure factor. In solid Ar or Kr, positive holes do not appear to be mobile, but in Xe crystals a hole mobility of about 2×10^{-2} cm^{2}sec^{-1}V^{-1} was found. The implications of these results are briefly discussed.

1. INTRODUCTION

THE rare gases Ne, Ar, Kr, and Xe form relatively simple liquids and solids, because the principal binding forces between the atoms are the weak and spherically symmetric van der Waals forces. In both liquid and solid, the local order is determined by the close packing of identical spheres; in the solid, the face-centered cubic configuration is stable.

There have been a considerable number of theoretical and experimental studies of the binding forces of the rare-gas solids (argon in particular) by x-ray diffraction techniques and thermodynamic means. This work is summarized in a number of well-known reviews.[1–3] However, the electrical properties, particularly of the solids, have so far received little attention. This is surprising, since it might be expected that the solid rare gases should behave as prototype solids as far as electronic transport phenomena are concerned. In the case of Ar, some relevant information is available from optical absorption measurements[4] and band-structure calculations.[5,6] These indicate a forbidden energy gap of about 13 eV and a conduction band 4 eV wide, with almost spherical energy surfaces, in which the effective electron mass is about $0.43m_e$. Furthermore, in a rare-gas crystal optical lattice modes of vibration do not occur, so that in a sufficiently pure and perfect specimen the low-field mobility should be determined solely by acoustic-mode scattering.

The only transport measurements that have been made on the rare-gas solids are those recently reported by Pruett.[7] In these experiments, charge carriers were generated near one crystal surface by α-particle excitation, and the transit time between the specimen electrodes was measured. The low yield per incident α particle restricted the measurements to a range of high applied fields (e.g., $E>15$ kV cm^{-1} for Ar, see Fig. 3). In this region, the electron drift velocity is practically field-independent, so that the results are difficult to interpret and do not lead to meaningful mobility values.

Far more is known about the transport properties of the rare-gas liquids. These "simple" fluids are of particular interest, from both the experimental and the theoretical points of view, because they form a system in which the generated excess electrons are in a quasifree state. This fact appears to have been first recognized by Davidson and Larsh[8] and by Hutchinson,[9] who investigated the properties of liquid Ar as a particle counter medium. Subsequent workers[10–12] have employed α-particle excitation to study the electron drift velocity in liquid Ar. Some of Swan's results[12] have been included in Fig. 4. For the reasons mentioned in connection with Pruett's work, this experimental method limited the measurements to applied fields above 10 kV cm^{-1}.

In the low-field region, Schnyders *et al.*[13,14] successfully used an electrical shutter technique to study the electron drift mobility in liquid Ar and Kr at fields below 200 V cm^{-1} (see Fig. 4). The experiments have

[1] G. L. Pollack, Rev. Mod. Phys. **36**, 748 (1964).
[2] E. R. Dobbs and G. O. Jones, Rept. Progr. Phys. **20**, 516 (1957).
[3] G. Boata, Cryogenics **4**, 65 (1964).
[4] G. Baldini, Phys. Rev. **128**, 1562 (1962).
[5] R. S. Knox and F. Bassini, Phys. Rev. **124**, 652 (1961).
[6] L. F. Mattheiss, Phys. Rev. **133**, A1399 (1964).
[7] H. D. Pruett, in Conference on Electronic Processes in Low-Mobility Solids, Sheffield, England, 1966 (unpublished).
[8] N. Davidson and A. E. Larsh, Jr., Phys. Rev. **77**, 706 (1950).
[9] G. W. Hutchinson, Nature **162**, 610 (1948).
[10] M. S. Malkin and H. L. Schultz, Phys. Rev. **83**, 1051 (1951).
[11] R. L. Williams, Can. J. Phys. **35**, 134 (1957).
[12] D. W. Swan, Proc. Phys. Soc. (London) **83**, 659 (1964).
[13] H. Schnyders, S. A. Rice, and L. Meyer, Phys. Rev. Letters **15**, 187 (1965).
[14] H. Schnyders, S. A. Rice, and L. Meyer, Phys. Rev. **150**, 127 (1966).

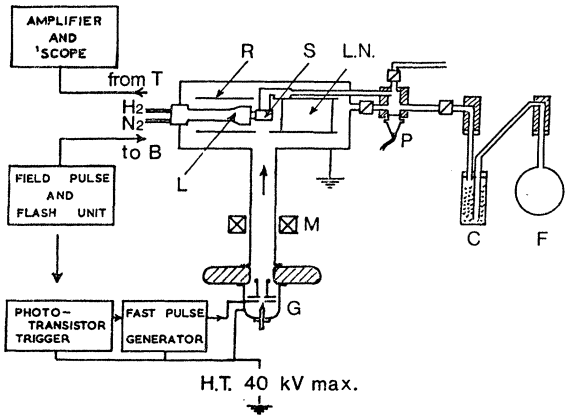

FIG. 1. Schematic diagram of the experimental arrangement. S: specimen chamber; R: radiation shield; L.N.: liquid-nitrogen reservoir; P: pressure transducer; C: charcoal trap; F: gas flask; L: miniature liquifier; M: magnetic lens; G: electron gun; T: specimen top electrode; B: specimen bottom electrode.

recently been extended by Halpern *et al.*[15] to fields of up to 1 kV cm^{-1}. Nevertheless, there still exists a wide intermediate field range in which, as a result of experimental limitations, no information is available. This introduces uncertainty in any comparison with the de-detailed theoretical predictions on the electron transport in rare-gas liquids which have recently been published.[16,17]

In the present work, an electron beam technique has been used to generate charge carriers in liquid and solid Ar, Kr, and Xe. This approach overcomes the limitations inherent in the previous methods and has made it possible to measure the electron drift velocity over a wide range of fields, from 10 V cm^{-1} to 100 kV cm^{-1}. Measurements on both solid and liquid can be made on a single specimen, and the electron mobility could therefore be studied during the change of state. A brief account of some of the results has been published.[18]

The aim of the present paper is twofold: first, to report meaningful mobility data for the above rare-gas crystals and liquids, and secondly, to attempt an interpretation of these results in the light of transport theory, particularly that recently put forward by Cohen and Lekner.[16,17]

2. EXPERIMENTAL METHOD

A schematic diagram of the complete system is shown in Fig. 1, and some of the more important features will now be discussed. The specimen (liquid or solid) is contained in a copper chamber S, about 2 cm in diameter, which is cooled by a miniature two-stage Joule-Kelvin liquifier L.[19] The temperature can be controlled and maintained to within 0.3°K from 20 to 300°K. The specimen chamber is partly surrounded by a cooled radiation shield R, and is mounted in a vacuum chamber in which a pressure of less than 10^{-5} Torr is maintained. In most of the recent experiments, the starting material was ultrapure gas[20] supplied in sealed 1-liter flasks. In some of the experiments, Ar from a metal cylinder [21]was also used. The gas inlet system was made of stainless steel and incorporated all-metal needle valves; indium O-rings were used for the demountable seals. The pressure of the gas in the specimen chamber was measured by the pressure transducer P fitted with a stainless-steel diaphragm. To obtain sufficiently long electron lifetimes for the low-field measurements, it was found necessary to further purify the gases, particularly with respect to their oxygen content. In the case of Ar and Kr, sufficient purification was achieved by passing the gas through the carefully outgassed and cooled charcoal trap C. To prevent contamination of the purified gas, the system was continuously pumped to a pressure below 10^{-5} Torr over as long a period as possible before each experiment. In the case of Xe, the purification was insufficient to allow measurements at very low fields. Alternative methods are being developed at present.

Figure 2 shows the detailed construction of the specimen chamber. The bottom electrode B, which also isolated the gas system from the surrounding vacuum, was a gold-plated Melinex (Mylar) foil, 6 μm thick, stretched tightly over a copper electron microscope mounting grid. This was supported by a perforated disk integral with the body of the chamber. The top electrode T was a thin copper disk supported by three fine "legs" of the same material. They were attached to a ring separated from electrode B by a ceramic spacer C. This design introduced some degree of flexibility, which reduced the strain suffered by the crystals when they were cooled below the temperature at which they were grown. In some experiments on the liquid and in some on the solid near the triple point, a more rigid top electrode, clamped to a ceramic spacer, was used. This facilitated the determination of the electrode spacing d, which in most of the experiments was in the range 100–600 μm.

The gas under investigation was condensed into the specimen chamber at temperatures and pressures not far from its triple point. When sufficient liquid had been condensed to fill the space between the two electrodes, the gas supply was shut off, and the system allowed to reach equilibrium. By careful adjustment of the cooling power of the cryostat, it was possible to grow the solid at a rate of less than 5 mm/h. In a number of subsidiary experiments, crystals were grown by the same method, and their surface examined in reflected light, when grain

[15] B. Halpern, J. Lekner, S. A. Rice, and R. Gomer, Phys. Rev. Letters (to be published).
[16] M. H. Cohen and J. Lekner, Phys. Rev. **158**, 305 (1967).
[17] J. Lekner, Phys. Rev. **158**, 130 (1967).
[18] L. S. Miller and W. E. Spear, Phys. Letters, **24A**, 47 (1967).
[19] "Cryotip," supplied by Air Products & Chemicals, Inc., Advanced Products Department, Allentown, Pa.

[20] B. O. C. Grade X gas: Ar$\not<$99.9995%, $N_2<5$ parts per 10^6 by volume (v.p.m.), $O_2<1$ v.p.m., $H_2<1$ v.p.m.; Kr$\not<$99.99%, Xe<50 v.p.m., $N_2<25$ v.p.m., O_2, H_2, $CO_2<5$ v.p.m.; Xe $\not<$99.99%, Kr<50 v.p.m., other impurities as for Kr.
[21] Air products, Ltd. Puragon: Ar$\not<$99.999%, $N_2<10$ v.p.m., $O_2<2$ v.p.m.

boundaries could be clearly seen. The average grain area was about 20 mm². This is about twice the effective area used in the transport measurements, so that the effect of grain boundaries was probably not significant.

The specimen was bombarded by 30–40-keV electron excitation pulses of 5–100-nsec duration. As indicated in Fig. 1, the electron gun together with the pulse generator connected to its modulator grid was kept at the negative high potential and was triggered by means of an optical link. The electrons entered the crystal through the bottom electrode and generated electron-hole pairs within a depth small compared to the electrode spacing d. The excitation pulses which had a repetition frequency of 50 pulses/sec were synchronized to occur during field pulses applied to the specimen electrode B. Depending on the polarity of the field, either type of charge carrier can be drawn across the specimen. The resulting displacement current was integrated, amplified, and observed on an oscilloscope. If the free charge carriers had a sufficiently long lifetime, their transit time t_t could be measured. This led directly to a value of the drift velocity $v=d/t_t$.

The electron beam technique has been successfully applied in studies of transport in thin films,[22] molecular crystals,[23] and II–VI compounds.[24] It makes it possible to generate in a controllable manner a sufficient number of charge carriers for experiments over a wide range of electric fields. With the present apparatus, transit times of about 25 nsec could be measured with an accuracy of ±10%. At the maximum charge sensitivity of the system, 1-cm deflection on the oscilloscope screen corresponded to the transit of 2×10^5 electrons.

In drift-mobility measurements, it is of importance to prevent the formation of appreciable surface or volume space charge which could seriously modify the electric field within the specimen. It is generally found that these effects are associated with the filling up of fairly deep-lying trapping centers. In the case of the rare-gas crystals, it is likely that such centers are mainly formed by oxygen-impurity molecules (see Sec. 3 B). Careful purification of the starting gas was therefore a most important part of the experimental procedure. In addition, it was found that polarization effects, which seemed to originate from the region near the bombarded electrode B, could be considerably reduced by arranging that only every fourth (or eighth) excitation pulse was accompanied by a field pulse. In this way, each electron transit was preceeded by 3 (or 7) space-charge neutralization pulses.

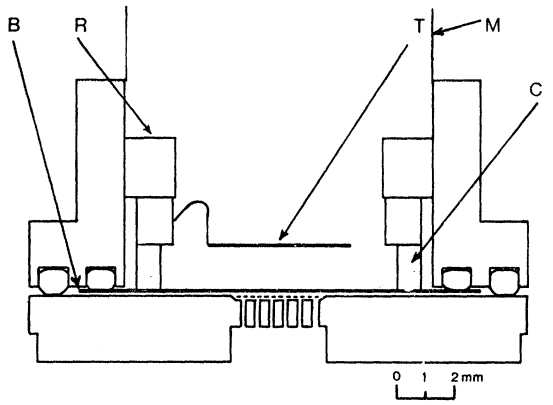

FIG. 2. Construction of specimen chamber. B: bottom electrode (gold-coated Mylar); T: top electrode (copper disc); C: ceramic spacer; R: Teflon clamping screw; M: Mylar tube. The demountable seals are indium rings.

TABLE I. Low-field electron mobilities μ_0 for the rare-gas solids and liquids at a temperature close to their triple points. The velocity of sound is denoted by u and the last column lists the saturation values of the drift velocity in terms of u.

	T(°K)	μ_0 (cm² sec⁻¹ V⁻¹)	u (10^5 cm sec⁻¹)	$(v/u)_{sat}$
Ar (solid)	82	1000	1.38[a]	10
Ar (liquid)	85	475	0.85[b]	9.4
Kr (solid)	113	3700	1.1[c]	8.0
Kr (liquid)	117	1800	0.7[d]	5.4
Xe (solid)	157	~4500	1.1[c]	5.0
Xe (liquid)	163	2200	0.65[d]	4.4

[a] D. J. Lawrence and F. E. Neale, Proc. Phys. Soc. (London) **85**, 1251 (1965).
[b] W. V. Dael *et al.*, Physica **32**, 611 (1966).
[c] Estimated from adiabatic compressibility (Ref. 1).
[d] C. C. Lim and R. A. Aziz, Can. J. Phys. **45**, 1275 (1967); and (private communication).

[22] W. E. Spear, Proc. Phys. Soc. (London) **B70**, 1139 (1957); **76**, 826 (1960).
[23] A. R. Adams and W. E. Spear, J. Phys. Chem. Solids **25**, 1113 (1964); D. J. Gibbons and W. E. Spear, *ibid.* **27**, 1917 (1966).
[24] W. E. Spear and J. Mort, Proc. Phys. Soc. (London) **81**, 130 (1963).

3. EXPERIMENTAL RESULTS

A. Drift-Velocity Measurements

Of the rare-gas solids and liquids investigated in this work, the most extensive measurements were made on Ar. Figures 3 and 4 show the results for a number of specimens of different thicknesses. The electron drift velocity v has been plotted as a function of the applied field on a log-log scale, and the results were obtained at temperatures near the triple point of Ar (at 82°K for the solid and 85°K for the liquid). Figures 5 and 6 give corresponding results for solid and liquid Kr and Xe, respectively.

The curves show three main features: First, in the low-field region, the drift velocity tends towards a linear field dependence as indicated by the dotted lines in some of the figures. The linear region is shown convincingly by the results for liquid Ar (Fig. 4), but in the case of Kr and Xe, the limit of linearity moves to progressively lower fields. In this range, the measurements are limited by the electron lifetime (see Sec. 3 B), which, particularly in solid Ar and Xe, restricted the experiments to fields above 100 V cm⁻¹. However, it

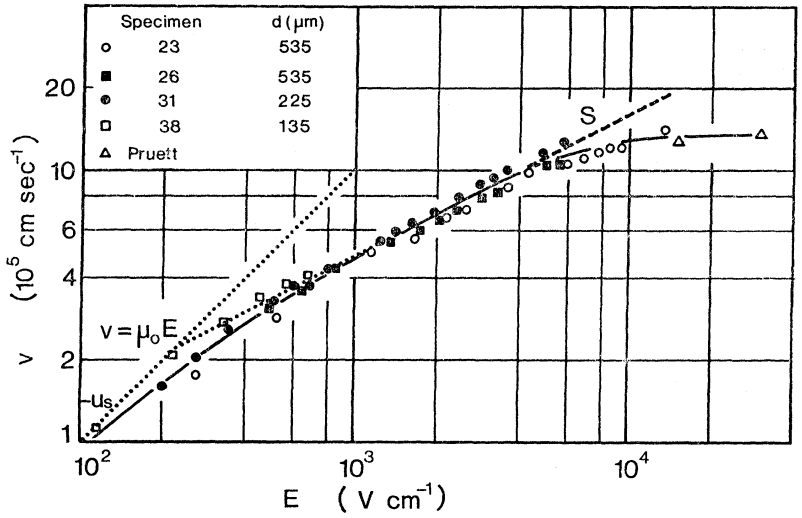

FIG. 3. The field dependence of the electron drift velocity in solid Ar at 82°K. The dotted lines show the extrapolated linear and $E^{1/2}$ regions intersecting at 1.5 u_s. Curve S was calculated from the Shockley theory (see Ref. 25) and fits the results up to $E \simeq 5$ kV cm^{-1}. The sound velocity in the solid is denoted by u_s.

was found that reliable and consistent values of the low-field electron mobility μ_0 could be deduced from the results by fitting the data to the Shockley hot-electron theory[25] (see Sec. 4 for further details). The advantage of this procedure lies in the fact that experimental points from a much wider field range can be used for the determination of μ_0.

The values of μ_0 so obtained are given in Table I together with the corresponding specimen temperature. It can be seen that the electron mobilities both in the liquids and the solids increase rapidly from Ar to Xe. In the case of solid Xe, only a lower limit of 3000 cm^2 sec^{-1} V^{-1} can be given at present. However, the Ar and Kr data show that μ_0 in the solid is about twice that in the liquid, so that for solid Xe one might expect a mobility approaching 4500 cm^2 sec^{-1} V^{-1}. The results obtained recently by Halpern *et al.*[15] for liquid Ar and by Schnyders *et al.*[14] for liquid Kr (at $E=1$ kV cm^{-1}) have been included in Figs. 4 and 5. They are in good agreement with our measurements obtained by an essentially different experimental method.

With increasing E, there is a transition to a second region in which v varies as $E^{1/2}$. This dependence is shown in the graphs by the broken line S. It is of interest, particularly with regard to the interpretation, that in all cases the transition from the linear to the $E^{1/2}$ region occurs when the drift velocity approaches the velocity of sound u in the medium. Values of u_s and u_l, referring to solid and liquid, have been marked on the velocity scale in Figs. 3–6 and are also included in Table I. As indicated in Fig. 3, the extrapolated E and $E^{1/2}$ lines intersect at about 1.5 u_s. The $E^{1/2}$ region is particularly well defined in solid Ar, where it extends from 1 to 5 kV cm^{-1}. In Kr and Xe it is much reduced.

The third feature common to all the curves is the complete saturation of the drift velocity in the high-field region. The ratio $(v/u)_{\text{sat}}$ is listed in Table I. Again, there is a systematic decrease in this quantity

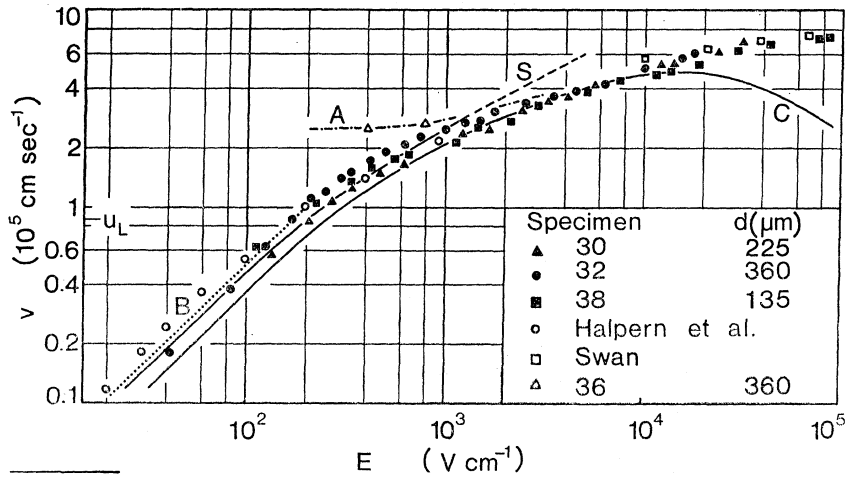

FIG. 4. The field dependence of the electron drift velocity in liquid Ar at 85°K. Curve S, calculated from Shockley theory; curve C, theory of Cohen and Lekner; curve B is corrected for multiple scattering and also indicates the linear field dependence. Curve A: typical results from a specimen with short electron lifetime ($\simeq$200 nsec). The sound velocity in the liquid is denoted by u_L.

[25] W. Shockley, Bell System Tech. J. 30, 990 (1951).

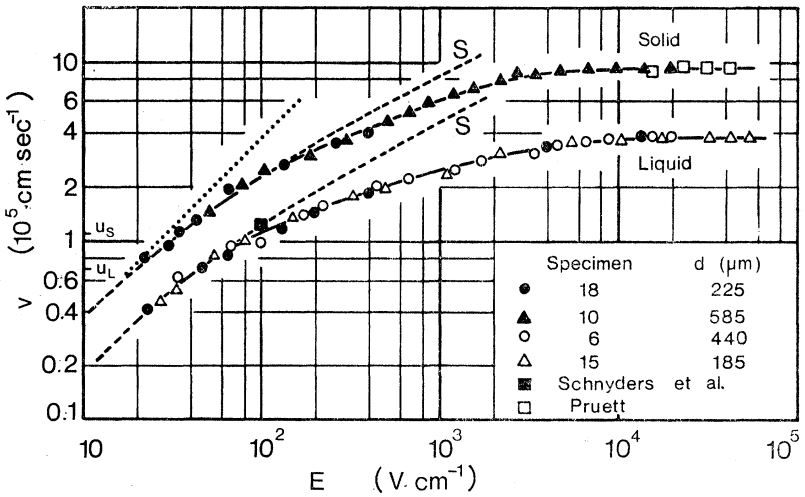

FIG. 5. The field dependence of the electron drift velocity in solid Kr (113°K) and liquid Kr (117°K). Dotted line: linear field dependence. Curves S: calculated from Shockley theory.

on going from Ar to Xe. $(v/u)_{sat}$ is always lower for the liquid as compared with the corresponding solid. The experimental points obtained by Pruett[7] for solid Ar, Kr, and Xe have been included in Figs. 2, 4, and 5 and are in good agreement with our results in the saturation region. The same applies to Swan's results[12] for liquid Ar plotted in Fig. 4.

In the case of Ar, a number of attempts have been made to investigate the temperature dependence of the low-field mobility in the solid. Considerable difficulties were experienced when the specimen was cooled below the temperature of growth. The transit signal decreased or disappeared altogether and strong polarization effects were observed. It is likely that this results from the contraction of the specimen which introduces strain and defects and may also lead to partial or complete loss of contact at the electrodes. Some of these difficulties were overcome by the use of the flexible-top electrode mentioned in Sec. 2. Figure 7 shows the temperature dependence of μ_0 for two Ar crystals down to 66°K. It can be seen that below about 80°K the results are consistent with a $T^{-3/2}$ temperature variation of μ_0. As expected, the low-field mobility is therefore controlled predominantly by acoustic-mode scattering. In specimens possessing long electron lifetimes, no deviations due to impurity scattering could be detected in the limited temperature range investigated. Near the triple point, the results show a smooth transition in low-field mobility during the change of state. The mobility ratio in solid and liquid Ar near the triple point is found to be $(\mu_0)_s/(\mu_0)_l \simeq 2.2$.

All the results presented so far refer to the electron drift velocity. During the course of the work, the mobilities of positive and negative ions in the liquid rare gases have also been measured, and the results are in reasonable agreement with previous work. Transit signals due to ionic motion are easily distinguishable from electronic signals as the mobilities differ by five orders of magnitude or more. It was of particular interest to look for hole transport in the rare-gas solids. In Ar and Kr, no positive signals could be detected, even after the sensitivity of the equipment had been increased by a factor of 10 at reduced bandwidth. However, in solid Xe well-defined hole transit signals could be observed. v-versus-E curves were linear up to the highest fields used and led to a hole mobility of about

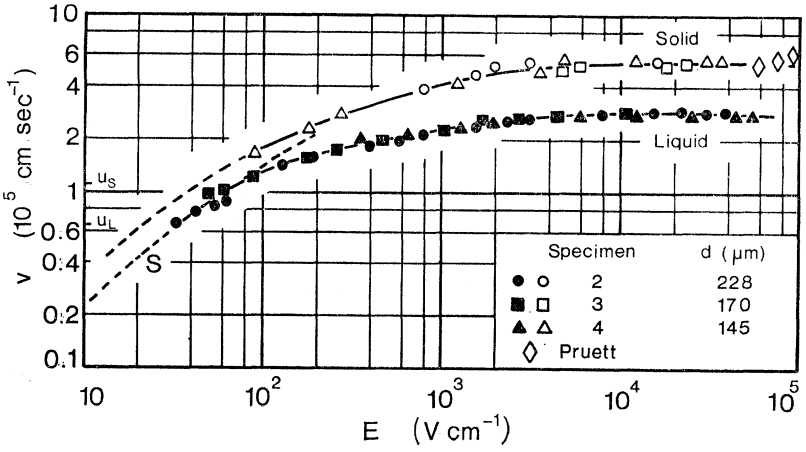

FIG. 6. The field dependence of the electron drift velocity in solid Xe (157°K) and liquid Xe (163°K). Curve S: calculated from Shockley theory.

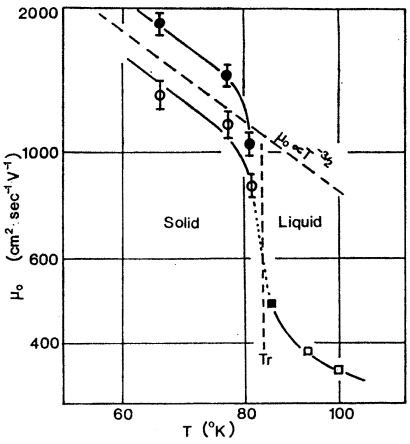

FIG. 7. The temperature dependence of the low-field mobility in Ar. Tr denotes the triple point. The two points denoted by open squares are from Ref. 13.

2×10^{-2} cm^2 sec^{-1} V^{-1} at 157°K in approximate agreement with the value quoted by Pruett.[7] The problem of hole transport in the rare-gas solids will be briefly discussed in Sec. 4.

B. Electron-Lifetime Measurements in Liquid Ar

Transit-time measurements are a very direct method for the determination of drift velocities, provided the lifetime τ of the drifting excess carriers with respect to deeper-lying trapping centers is much longer than the transit time t_t. If this condition is satisfied, the integrated charge displacement $q(t)$ observed on the oscilloscope will have the form shown by trace 1 (insert to Fig. 8) which then leads to a sharply defined value for t_t. The results shown in Figs. 3–6 were all obtained on long-lifetime specimens in which the condition $\tau>t_t$ was satisfied, down to the lowest fields.

If, however, the density of deep trapping centers is sufficiently high so that $\tau\sim t_t$ in the low-field region, then an appreciable number of carriers will be lost during transit, and the oscilloscope trace has the form indicated by 2. It is then useful to measure the time t', defined by the intersections of the tangents at $t=0$ and $t>t_t$. Observations of this kind form a convenient method for the determination of carrier lifetime in a particular specimen. This approach has previously been used in a study of the hole lifetime in CdS[24] and it can be shown that

$$t'=\tau[1-\exp(-t_t/\tau)]. \tag{1}$$

Extrapolation to the low-field limit (i.e., $t_t=\infty$) will therefore lead to a value of τ. This procedure is illustrated in Fig. 4 by curve A, which represents a plot of d/t' versus E for a relatively short-lifetime specimen ($\tau\simeq200$ nsec). From a knowledge of t' and t_t, it is now possible to investigate the lifetime as a function of E. The experiments showed that τ is an increasing function of E, a fact observed by Swan[12] in a field range between 15 and 60 kV cm^{-1}. Swan measured the electron-attachment coefficient $\eta=1/v\tau$ for oxygen impurities in liquid Ar as a function of applied field and oxygen concentration P_0. Figure 8 is a graph of $v\tau P_0$ versus E, and the solid part of the line is defined by Swan's results. Our values for $v\tau P_0$, obtained from drift-velocity and lifetime measurements, will lie on the extrapolated straight line provided P_0 is chosen as 2 parts per 10^6 by volume (v.p.m.). This is equal to the stated maximum oxygen content[21] of the cylinder gas from which the particular specimen was prepared without further purification. On the other hand, liquid-Ar specimens prepared from gas purified further in the charcoal trap led to τ values as high as 10μ sec. According to Fig. 8, this should correspond to an oxygen impurity content of about 4×10^{-2} v.p.m.

These results confirm the conclusion of previous workers[13,14] that the electron lifetime in liquid Ar (and possibly Kr and Xe) is predominantly determined by oxygen impurities. It is very likely that the same applies to the solids.

4. DISCUSSION

There is little doubt that the nonlinear field dependence of the drift velocity shown by the curves in Sec. 3 A is caused by the "heating up" of the electron distribution. It is therefore of some interest to determine how far the well known hot-electron theory of Shockley[25] can account for these results. The Shockley theory describes the energy distribution of the hot electrons by an effective temperature T_e, on the assumption that the distribution remains Maxwellian. The ratio $T_e/T=\gamma$, where T is the lattice temperature, is determined by equating the rate of energy gain by the electron system from the applied field to the rate of loss by acoustic scattering. This leads to

$$\gamma^2-\gamma=\frac{3\pi}{32}\left(\frac{\mu_0E}{u}\right)^2. \tag{2}$$

The drift velocity is given by

$$v=\gamma^{-1/2}\mu_0E. \tag{3}$$

At low fields, $\gamma\simeq1$ and $v\simeq\mu_0E$. With increasing field, the theory predicts a transition to an $E^{1/2}$ region; the intersection of the extrapolated parts of the two curves should lie at $v=1.51u$. An attempt has been made to fit the theory to all the experimental results, except those for solids Xe. Curves S in Figs. 3–6 have been calculated from Eq. (2) and (3) with the appropriate values of u. μ_0 was obtained from the best fit to the experimental points. It can be seen that the theory is in good agreement with the solid-Ar results (Fig. 3), from the lowest field point near 100 V cm^{-1} up to 5 kV cm^{-1}, where the $E^{1/2}$ curve, indicated now by the dashed line, deviates from the experimental points. At this field value, the electron temperature is about $17T$, according to Eq.

(2). In liquid Ar and particularly in Kr and Xe, the validity of the Shockley theory is confined to a very much smaller range of fields, and it clearly cannot account for the observed velocity saturation.

Cohen and Lekner[16] have recently developed a more detailed hot-electron theory valid equally for gases, liquids, and solids. The significant advance of this treatment lies in the fact that it takes account of the structure of the medium containing the electrons. The theory distinguishes between two mean free paths for the electrons: one describing the energy loss to acoustic phonons which is independent of the structural properties, the other related to the momentum transfer and dependent on the structure through the structure factor $S(K)$. At the lower applied fields, the velocities predicted by this theory do not differ substantially from those calculated from the Shockley theory. However, at higher fields the effect of structure becomes important in the treatment of liquids and solids and leads to an increase in the scattering cross section.

Lekner[17] carried out detailed calculations in the case of liquid Ar, and curve C in Fig. 4 shows the results. The agreement with the experimental data is extremely good over most of the field range, particularly as the theory contains no adjustable parameters. At the low-field end, curve B shows C corrected for multiple scattering.[15] At high fields, the theory suggests a maximum in the v-versus-E curve rather than the complete saturation which is characteristic of all our experimental results. Lekner suggests two reasons which could explain this discrepancy. First, the theoretical cross sections are inaccurate at these electron energies, and secondly, the experimental results are affected by impurities. Lekner estimates that impurity concentrations in excess of 10 v.p.m. could modify the high-field drift velocity by inelastic scattering which would reduce the mean electron energy. In view of our purification procedure and the independent evidence obtained from

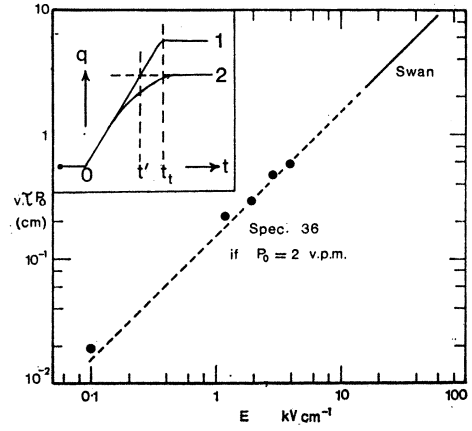

FIG. 8. The product of the electron capture distance $v\tau$ and the oxygen impurity content P_0 (in v.p.m.) plotted against the applied field E. The solid part of the line was obtained from the data of Swan (see Ref. 12). Insert: Observed pulse shapes. Trace 1: $\tau \gg t_t$; trace 2: $\tau \sim t_t$.

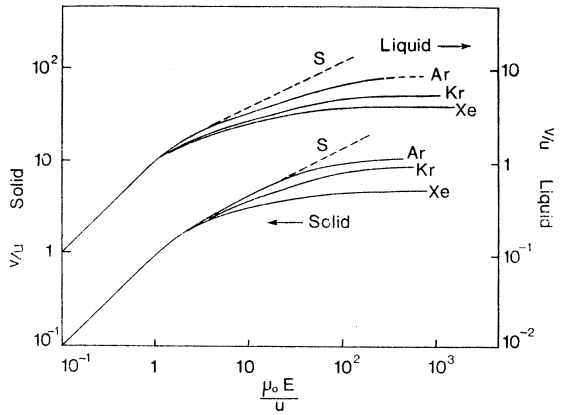

FIG. 9. Graph correlating the drift-velocity results for liquid and solid rare gases. Note that for clarity the results for the solids and liquids refer to different vertical scales. All the results would lie on curve S if the Shockley theory were obeyed.

lifetime measurements (Sec. 3 B), it would seem most unlikely that such high impurity levels were present in our liquid Ar. It appears therefore that the discrepancies in the high-field region are associated with the inaccuracy of the cross-section calculation, or possibly with basic approximations made in the theory.

In the low-field limit, Lekner's theory leads to

$$\mu_0 = \tfrac{2}{3}(2/\pi mkT)^{1/2} e/4\pi a^2 n S(0)\,, \qquad (4)$$

where a denotes the scattering length, n the density of atoms, and $S(0)$ the long-wavelength limit of the structure factor. The latter is given in terms of the isothermal compressibility χ_T by $S(0) = nkT\chi_T$. The ratio of low-field mobilities in the solid and liquid is therefore

$$(\mu_0)_s/(\mu_0)_L = (n_L/n_s)^2 (a_L/a_s)^2 (\chi_T)_L/(\chi_T)_s\,. \qquad (5)$$

On the assumption that the scattering lengths in the liquid and solid are approximately the same, Eq.(5) predicts a ratio of $(\mu_0)_s/(\mu_0)_L = 2.0$ in the case of Ar. This is in good agreement with the experimentally determined value of 2.2. Values of χ_T for liquid Kr and Xe are not available, and it was therefore not possible to make similar calculations in these cases.

An interesting comparison of all the results in the region of higher fields is shown in Fig. 9. We have plotted v/u against $\mu_0 E/u$, using the sound velocities listed in Table I. (For clarity, the curves for the liquids have been plotted on a vertical scale displaced from that used for the solids.) The graph illustrates the similarity between the solid and liquid results and the progressive change in behavior from Ar to Xe. With the particular variables chosen, all the curves should coincide with curve S as long as the Shockley theory applies.

An attempt was made to determine whether the onset of deviations from curve S and the saturation behavior could be correlated in any way with the shape of the calculated structure-factor curves at the lower K values. In the computations, based on the solution of

the Percus-Yevick equations,[26] we used the hard-core diameters recently obtained by Ashcroft[27] for the rare-gas liquids. Curves of $S(K)/S(0)$ versus K were plotted in the range of interest up to about $K=2$ Å^{-1}. At any given K, the values of $S(K)/S(0)$ increased in the order Ar, Kr, Xe, which might, at least qualitatively, explain the sequence of the saturation values shown in Fig. 9. Clearly, calculations based on the Cohen-Lekner theory are necessary before any more detailed comparisons can be made.

A number of calculations have also been made to evaluate the possible effect of charged impurity scattering of the interpretation of the results. One would expect this scattering mechanism to lead to additional loss of forward momentum in the low-field region, but its effect should become negligible with increasing electron temperature. Acoustic and charged impurity scattering were combined using the integrals tabulated by Dingle *et al.*[28] The results, which are in general agreement with those of Matz and Garcia-Molliner[29] for silver halides, show two main features: (a) a reduction in μ_0, and (b) a shift in the intersection of the extrapolated linear and $E^{1/2}$ regions towards higher-field values, which effectively causes an extension of the linear part of the drift-velocity curve. For instance if in the case of solid Ar it is assumed that the mobility determined by charged impurity scattering is $6\mu_0$, then μ_0 will be reduced to 600 cm^2 sec^{-1} V^{-1}. The intersection of the two regions will now be at $v\simeq 3u_s$ instead of the 1.5 u_s expected from acoustic scattering alone. Such appreciable deviations from the Shockley theory have not been found in any of the results from long-lifetime specimens, and it is reasonable to conclude that in these cases impurity scattering has a negligible effect.

Finally, the hole transport in solid Xe and its absence in Kr and Ar require some comment. Recent band-structure calculations[30] indicate that the valence band in crystalline Xe is about 0.5 eV wide. A hole drift mobility of 2×10^{-2} cm^2 sec^{-1} V^{-1} implies a fairly strong localization of the excess hole and suggests that the small polaron theory[31] should be applicable. Two transport mechanisms should thus be possible in principle: an intermolecular hopping conduction, or transport in a narrow polaron band. Experiments on the temperature dependence of the hole mobility are in progress, aimed at distinguishing between these two mechanisms.

The calculated width[6] of the valence band in solid Ar is of the same order as for Xe, and the complete absence of positive charge transport is puzzling. It is possible that the strong localization of the excess hole is connected with a center of the type Ar_2^+.[32] Its stability is likely to be fairly temperature-dependent, so that in solid Ar at 82°K the formation of such centers could completely immobilize the positive holes generated in the region near to the bottom electrode. This would explain the need for space-charge neutralization (Sec. 2). On the other hand, the Xe_2^+ center may at 157°K be sufficiently unstable to allow hole transport to take place either in a polaron band or by a hopping mechanism.

5. CONCLUSIONS

(1) The rare-gas solids possess comparatively high electron mobilities which range from 1000 cm^2 sec^{-1} V^{-1} in solid Ar (82°K) to about 4500 cm^2 sec^{-1} V^{-1} in Xe (157°K). Near the triple point, the electron mobility in the rare-gas liquids is about one half of that in the corresponding solid.

(2) Measurements on Ar crystals to 66°K indicate that the low-field mobility is determined by acoustic scattering. In crystals prepared from highly purified gas, there is no evidence for charged impurity scattering.

(3) The results of electron-lifetime measurements suggest that the lifetime is determined predominantly by oxygen impurities.

(4) When the drift velocity approaches the velocity of sound in the medium, pronounced hot-electron effects are observed in both liquids and solids. The results fit the Shockley theory[25] over a wide range of fields in the case of Ar, but in Kr and Xe the range is much more limited.

(5) In the high-field region the electron drift velocity in solids and liquids approaches complete saturation. The detailed theory of Cohen and Lekner[16] fits the liquid Ar results extremely well. The discrepancy at very high fields appears to be due to insufficient accuracy in the calculation of the scattering cross section.

(6) A comparison of v-versus-E curves for liquid and solid Ar, Kr, and Xe shows a very similar general behavior. Individual differences between the curves on approaching the saturation region are thought to be associated with the detailed shape of the structure-factor–versus–K curves.

(7) The transport of generated holes was not observed in solid Ar or Kr. In Xe crystals, a hole mobility of about 2×10^{-2}cm^2 sec^{-1} V^{-1} was obtained which might be associated with hopping or with transport in a polaron band.

ACKNOWLEDGMENTS

The authors would like to thank Professor S. A. Rice and Professor M. H. Cohen for reports of their papers. We are indebted to Dr. J. Lekner for helpful information and permission to include his calculated curve in Fig. 4. The support of this work by a Scientific Research Council Research Grant and by a Research Studentship is gratefully acknowledged.

[26] N. W. Ashcroft and J. Lekner, Phys. Rev. **145**, 83 (1966).
[27] N. W. Ashcroft, Physica **35**, 148 (1967).
[28] R. B. Dingle, D. Arndt, and S. K. Roy, Appl. Phys. Sci. Res. **B6**, 155 (1956).
[29] D. Matz and F. Garcia-Molliner, J. Phys. Chem. Solids **26**, 551 (1965).
[30] N. H. Reilly (private communication).
[31] T. Holstein, Ann. Phys. (N. Y.) **8**, 343 (1959).
[32] We are indebted to Professor R. Knox for this suggestion.